Article

Silica Encapsulation of Hydrophobic Optical NP-Embedded Silica Particles with Trimethoxy(2-Phenylethyl)silane

Eunil Hahm [1], Ahla Jo [1], Eunji Kang [1], Kwanghee Yoo [1], Minsup Shin [1], Jaehyun An [1], Xuanhung Pham [1], Hyungmo Kim [1], Homan Kang [2], Jaehi Kim [1,*] and Bonghyun Jun [1,*]

[1] Department of Bioscience and Biotechnology, Konkuk University, Seoul 05029, Republic of Korea; dnjzj159159@konkuk.ac.kr (M.S.); wogus4067@naver.com (J.A.)
[2] Gordon Center for Medical Imaging, Department of Radiology, Massachusetts General Hospital, Harvard Medical School, Boston, MA 02114, USA
* Correspondence: susia45@gmail.com (J.K.); bjun@konkuk.ac.kr (B.J.)

Abstract: Nanoparticles (NP) with optical properties embedded silica particles have been widely used in various fields because of their unique properties. The surfaces of optical NPs have been modified with various organic ligands to maintain their unique optical properties and colloidal stability. Among the surface modification methods, silica encapsulation of optical NPs is widely used to enhance their biocompatibility and stability. However, in the case of NPs with hydrophobic ligands on the surface, the ligands that determine the optical properties of the NPs may detach from the NPs, thereby changing the optical properties during silica encapsulation. Herein, we report a generally applicable silica encapsulation method using trimethoxy(2-phenylethyl)silane (TMPS) for non-hydrophilic optical NPs, such as quantum dots (QDs) and gold NPs. This silica encapsulation method was applied to fabricate multiple silica-encapsulated QD-embedded silica NPs ($SiO_2@QD@SiO_2$ NPs; QD^2) and multiple silica-encapsulated gold NP-embedded silica NPs labeled with 2-naphthalene thiol ($SiO_2@Au_{2-NT}@SiO_2$). The fabricated silica-encapsulated NPs exhibited optical properties without significant changes in the quantum yield or Raman signal intensity.

Keywords: silica encapsulation; silica-encapsulated nanoparticles; trimethoxy(2-phenylethyl)silane

1. Introduction

Nanoparticles (NPs) with optical properties, such as plasmonic NPs and fluorescent quantum dots (QDs), have been extensively utilized in various fields, including biomedical imaging, drug delivery, sensing, catalysis, and optoelectronics [1–4]. To improve the biocompatibility of NPs and impart them with additional merits, researchers have focused on a silica encapsulation method for optical NPs [5–9]. Silica-encapsulated NPs have several advantages over organic ligand-coated NPs. First, the outer silica shell prevents direct contact between the encapsulated NPs and the external environment; thus, the silica-encapsulated NPs remain unaffected by degradation or oxidation and do not exhibit cytotoxicity [10,11]. Second, the silica shell enhances the hydrophilicity of the NPs and prevents their aggregation under physiological conditions. Unlike commonly used hydrophobic organic ligands, such as oleic acid or trioctylphosphine oxide, silica-encapsulated NPs are hydrophilic with silanol groups in the silica shell. Finally, the silica shell provides flexibility for surface modification. Silanol groups can easily react with various silanol precursors with functional groups, such as amine or thiol groups; therefore, various functional groups like amine or thiol groups can be introduced with other silylether-containing compounds, such as 3-aminopropyl triethoxysilane (APTES), 3-chloropropyl trimethoxysilane (CPTMS), 3-glycydoxypropyl trimethoxysilane (GPTS), or 3-mercaptopropyl trimethoxysilane (MPTS) [12–15].

Embedding optical NPs into silica particles has significant potential in bio applications as it enables enhanced and/or tunable optical properties and ease of handling. Focusing

on these merits, we have reported various types of silica-encapsulated NPs, including silica templates and surface modification methods using MPTS and tetraethyl orthosilicate (TEOS) [16–21]. Because the thiol group of MPTS has a high affinity for optical NPs, such as Au or QDs, silica precursors can be easily introduced on the surface of the optical NPs, and easily forming a silica shell. Their unique optical properties are retained after silica shell coating, and they have been successfully employed in biological experiments. However, the fabrication method using MPTS has potential disadvantages owing to its encapsulation mechanism. When MPTS attaches to the surface of QDs via ligand exchange, the crystal structure of the QDs may be damaged, causing a significant decrease in the quantum yield (QY) [22]. In the case of Ag or Au NPs labeled with Raman labeling compounds (RLCs), MPTS can replace the RLCs. Consequently, the number of RLCs reduces after silica encapsulation, and the signal intensity of the Raman scattering decreases significantly. To avoid these problems, it is necessary to develop a silica encapsulation method without thiol-containing silica precursors that directly attach to the surface of optical NPs.

Trimethoxy(2-phenylethyl)silane (TMPS) is a silane derivative containing one phenylethyl group and three methoxy groups attached to a silicon atom. Therefore, it can be used to introduce a silane group into composite materials because the phenylethyl group of TMPS can adhere to hydrophobic surfaces. Although TMPS has been used for the silica coating of QD NPs on silica templates, it has been limited to hydrophobic silica and QDs [23]. Owing to the high demand for silica coatings for composite structures with hydrophobic surfaces, it is necessary to develop general methods capable of coating non-hydrophilic surfaces with silica to expand their applicability.

This paper presents a generally applicable method for encapsulating optical NP-embedded silica NPs using TMPS. By substituting the reagent for silica encapsulation from MPTS to TMPS, which cannot interact directly with optical NPs, the ligand exchange or detachment of the RLCs is inhibited during the silica encapsulation step. Compared with previously reported silica-encapsulated optical NPs, such as silica-encapsulated multiple QD-embedded silica NPs ($SiO_2@QD@SiO_2$ NPs; QD^2) or metal NPs with RLC-embedded silica particles ($SiO_2@Au_{2\text{-}NT}@SiO_2$), the optical properties, such as the QY or SERS signal intensity, were only slightly reduced after silica encapsulation. Finally, the thickness of the silica shell can be controlled by adjusting the amount of TEOS used for additional silica shell formation.

2. Materials and Methods

2.1. Influence of Silica

For this study, tetraethylorthosilicate (TEOS), 3-mercaptopropyl trimethoxysilane (MPTS), chloroform, tetrakis(hydroxymethyl)-phosphonium chloride (THPC), polyvinylpyrrolidone (PVP, MW ~40,000), gold(III) chloride trihydrate ($HAuCl_4 \cdot 3H_2O$), ascorbic acid (AA), 3-aminopropyl triethoxysilane (APTES), 2-naphthalenethiol (2-NT), and trimethoxy(2-phenylethyl)silane (TMPS) were purchased from Sigma Aldrich (St. Louis, MO, USA). Dichloromethane and sodium hydroxide (NaOH) were purchased from Samchun (Pyeongtaek, Republic of Korea). Ethyl alcohol (EtOH, 99.9% purity) and aqueous ammonium hydroxide (NH_4OH, 27% purity) were purchased from Daejung (Siheung, Republic of Korea). The quantum dots (QDs) were purchased from Zeus (Osan, Republic of Korea). These materials did not undergo any purification after purchase.

Transmission electron microscopy (TEM) images of the NPs were obtained using the JEM-2010 system (JEOL, Tokyo, Japan). The ultraviolet–visible (UV-Vis) light absorbance spectra of the NPs were obtained using an Optizen Pop UV/Vis spectrophotometer (Mecasys, Daejeon, Republic of Korea). The photoluminescence (PL) emission spectra of the NPs were obtained using a Cary Eclipse spectrophotometer (Agilent Technologies, Santa Clara, CA, USA). The quantum yield (QY) of NPs was measured using a QE-2000 instrument (Otsuka Electronics, Osaka, Japan). Raman spectra were obtained using a DXR Raman microscope (Thermo Fisher Scientific, Madison, WI, USA) equipped with a 780 nm diode laser. The samples prepared in solution were subjected to Raman measurements

using capillary tubes. Each spectrum was measured in the range of 500–1800 cm^{-1} with a spectral resolution of 0.5 cm^{-1}, and the SERS signals were collected with a backscattering geometry using a ×10 objective lens.

2.2. Preparation of Thiol- or Amine-Functionalized SiO$_2$NPs (SiO$_2$-SH or SiO$_2$-NH$_2$)

Approximately 150 nm of silica NPs (SiO$_2$ NPs) were synthesized using the Stöber method with modification [24]. First, 40 mL of EtOH was mixed with 1 mL each of distilled water and 1.6 mL of TEOS. Subsequently, the mixture was mixed after adding 3 mL of NH$_4$OH for 20 h at 25 °C. The SiO$_2$ NPs were washed with EtOH several times by using centrifugation at 8500 rpm for 15 min and redispersed in EtOH.

To introduce the thiol groups onto the surface of SiO$_2$ NPs, 10 μL of MPTS, 10 μL of distilled water, and 2.5 μL of NH$_4$OH were added into 980 μL of SiO$_2$ mixture in EtOH (1 mg/mL). The mixture was incubated for 1 h at 50 °C, and thiol-functionalized SiO$_2$ NPs were washed with EtOH several times by using centrifugation at 8500 rpm for 15 min. After washing, the thiol-functionalized SiO$_2$ NPs were redispersed in EtOH (10 mg/mL). To introduce amine groups on the surface of the SiO$_2$ NPs, the same fabrication process was used, except that the MPTS was substituted with the same amount of APTES. The prepared 980 μL of SiO$_2$ mixture (1 mg/mL) was stirred with 10 μL of APTES, 10 μL of distilled water, and 2.5 μL of NH$_4$OH for 1 h at 50 °C. After the reaction, the amine-functionalized SiO$_2$ NPs were washed with EtOH several times by using centrifugation at 8500 rpm for 15 min and redispersed in EtOH (10 mg/mL).

2.3. Preparation of SiO$_2$@QD

The prepared SiO$_2$-SH in EtOH (10 mg/mL, 1 mL) was mixed with 4 mL of dichloromethane and 6 mg of red QDs (100 mg/mL in toluene). The mixture was stirred using a rotator for 6 h at 50 rpm. To minimize particle aggregation, the reaction solution was sonicated for 1 min every 60 min. Subsequently, the SiO$_2$@QDs mixture was washed using EtOH three times by using centrifugation at 7000 rpm for 10 min, and the washed particles were redispersed in EtOH after washing for storage.

2.4. Preparation of SiO$_2$@QD@TMPS

Solvent exchange was performed to introduce TMPS to the surface of SiO$_2$@QDs. The solvent of the SiO$_2$@QD mixture was removed by using centrifugation at 7000 rpm for 10 min, and the SiO$_2$@QD was dispersed in 20 mL of ethanol/chloroform (2:1, in terms of the volume ratio) mixture. To this mixture, 1.2 mL of distilled water and 0.8 mL of NH$_4$OH were added while stirring. Subsequently, 140 μL of TEOS and 60 μL of TMPS were added to the mixture, and the mixture was stirred for 6 h at 25 °C. To reduce particle aggregation, the reaction mixture was sonicated every 1 h. The reaction mixture was washed several times with EtOH by using centrifugation at 7000 rpm for 10 min, and the washed particles were redispersed in 5 mL of EtOH.

2.5. Preparation of SiO$_2$@QD@TMPS-SiO$_2$

To encapsulate SiO$_2$@QD@TMPS with a silica shell, 50 μL of D.W, 50 μL of TEOS, and 50 μL of NH$_4$OH were added to the SiO$_2$@QD@TMPS mixture and stirred using a rotator for 20 h at 25 °C. The final particles were washed by using centrifugation at 7000 rpm for 10 min and redispersed in EtOH.

For varying the thickness of the silica shell, the outer layer of SiO$_2$@QD@TMPS, was accomplished by adjusting the amount of TEOS used. The silica encapsulation process of the outer layer of SiO$_2$@QD@TMPS was conducted by adjusting the amount of TEOS to 25, 50, and 100 μL, respectively, while leaving the other reaction conditions unchanged. After the silica encapsulation process, the SiO$_2$@QD@TMPS-SiO$_2$ mixture was washed several times with EtOH by using centrifugation at 7000 rpm for 10 min, and the washed particles were dispersed in EtOH.

2.6. Preparation of SiO$_2$@Au

SiO$_2$@Au was fabricated based on the method detailed previously [25,26]. First, the 3–5 nm size of Au NPs were fabricated using the THPC method [27]. In detail, 1.5 mL of 0.2 M NaOH solution, 12 μL of THPC, and 1.5 mL of 50 mM HAuCl$_4$·3H$_2$O solution were added sequentially into 47.5 mL of deionized water. The mixture was stirred for 1 h at room temperature, and after the reaction, the mixture was stored in a 4 °C refrigerator for at least two days prior to use. To attach Au NPs onto the silica template, 10 mL of Au NP mixture was mixed in 200 μL of prepared SiO$_2$–NH$_2$ (10 mg/mL). The mixture was incubated overnight at room temperature. Silica NPs with Au NPs embedded as a seed (SiO$_2$@ seed Au NPs) were obtained after washing with EtOH several times by using centrifugation at 8000 rpm for 10 min and were redispersed in 2 mL of PVP solution (0.1%, *w/v*).

For the growth of Au NPs on SiO$_2$@ seed Au NPs, 10 mg of PVP was dissolved in 9.8 mL of deionized water, and 200 μL of SiO$_2$@seed Au NPs were mixed with this solution. To this solution, 20 μL of 10 mM HAuCl$_4$·3H$_2$O solution and 40 μL of 10 mM ascorbic acid solution were added every 5 min, until the final concentration of Au^{3+} reached 500 μM. After the reaction, Au NP-embedded silica NPs (SiO$_2$@Au NPs) were obtained by washing with EtOH several times by using centrifugation at 8000 rpm for 10 min and redispersed in EtOH to adjust the concentration of NPs to 0.1 mg/mL.

2.7. Preparation of 2-NT Labeled SiO$_2$@Au NPs (SiO$_2$@Au$_{2\text{-}NT}$ NPs)

First, 1 mL of 2 mM 2-NT was prepared using an EtOH/DMF mixture (1:9 volume ratio) as the Raman labeling compound (RLC) solution. SiO$_2$@Au mixture (1 mL) was transferred into a microtube, and the solvent of mixture was decanted after centrifugation at 8000 rpm for 10 min. The particles were redispersed in the prepared RLC solution, and the mixture was shaken for 1 h at room temperature. After the reaction, SiO$_2$ @Au$_{2\text{-}NT}$ NPs were obtained after washing with EtOH several times by using centrifugation at 8000 rpm for 10 min and then redispersed in 1 mL of EtOH to adjust the particle concentration at 0.1 mg/mL.

2.8. Silica Encapsulation of SiO$_2$@Au$_{2\text{-}NT}$ NPs (SiO$_2$@Au$_{2\text{-}NT}$@SiO$_2$ NPs)

Silica encapsulation of SiO$_2$@Au$_{2\text{-}NT}$ NPs was conducted via a similar method with SiO$_2$@QD NPs. The solvent of SiO$_2$@Au$_{2\text{-}NT}$ NP mixture (500 μL, 0.05 mg) was removed after centrifugation at 8000 rpm for 10 min, and SiO$_2$ @Au$_{2\text{-}NT}$ NPs were dispersed in 200 μL of EtOH/CHCl$_3$ (2:1, in terms of the volume ratio) mixture. To this mixture, 12 μL of deionized water, 8 μL of NH$_4$OH, 1.4 μL of TEOS, and 0.6 μL of TMPS were added sequentially. While incubating the mixture at room temperature, the mixture was sonicated every 1 h to prevent the aggregation of particles. The reaction was continued for 6 h, and TMPS-introduced SiO$_2$@Au$_{2\text{-}NT}$ NPs (SiO$_2$@Au$_{2\text{-}NT}$@TMPS NPs) were washed with EtOH several times by using centrifugation at 8000 rpm for 10 min. After washing, SiO$_2$@Au$_{2\text{-}NT}$@TMPS NPs were dispersed in 2.5 mL of EtOH, and 25 μL of deionized water and 25 μL of NH$_4$OH were added to the mixture. To this mixture, 5 μL of TEOS was added every 30 min, five times in total. The reaction was kept for an additional 18 h at room temperature. SiO$_2$@Au$_{2\text{-}NT}$@SiO$_2$ NPs were obtained after washing with EtOH several times by using centrifugation at 8000 rpm for 10 min and were redispersed in 1 mL of EtOH.

3. Results and Discussion

3.1. Fabrication of Silica-Encapsulated QD-Embedded Silica NPs with TMPS (SiO$_2$@QD@TMPS-SiO$_2$)

Figure 1 shows the fabrication process of the silica-encapsulated QD-embedded silica NP with TMPS (SiO$_2$@QD@TMPS-SiO$_2$). Compared to previous attempts used to fabricate silica–QD hybrid NPs via hydrophobic interactions by introducing octadecyl groups on their surfaces, silica NPs (SiO$_2$ NPs) fabricated using the Stöber method were functionalized

with thiol groups. Because thiol groups on the SiO_2 NP surface do not interact with each other, SiO_2 NPs do not undergo aggregation during the fabrication process, whereas the previous attempts have caused aggregation of silica NPs due to the hydrophobic interaction between the octadecyl groups. The average size of the SiO_2 NPs was 175.0 ± 4.04 nm (Figure 2a and Figure S1). As shown in Figure 2b, the QDs were densely embedded onto the surface of the SiO_2 NPs, in which thiol groups were introduced, via the ligand exchange method. To encapsulate the SiO_2@QD with silica, TMPS was used as the silica precursor with a hydrophobic moiety. Although the 2-phenylethyl group was shorter than the octadecyl group and more difficult to interact with the oleyl group owing to the difference in the molecular structure, the hydrophobic interaction between the oleyl group and the 2-phenylethyl group was sufficiently strong to surround the SiO_2@QDs with TMPS (Figure 2c). To increase the thickness of the silica shell at the outer layer of the SiO_2@QD@TMPS, additional silica encapsulation was provided using tetraethyl orthosilicate (TEOS) as a silica source (Figure 2d). As shown in Figure 2b–d, there was no significant leaching of the QDs during the silica encapsulation process.
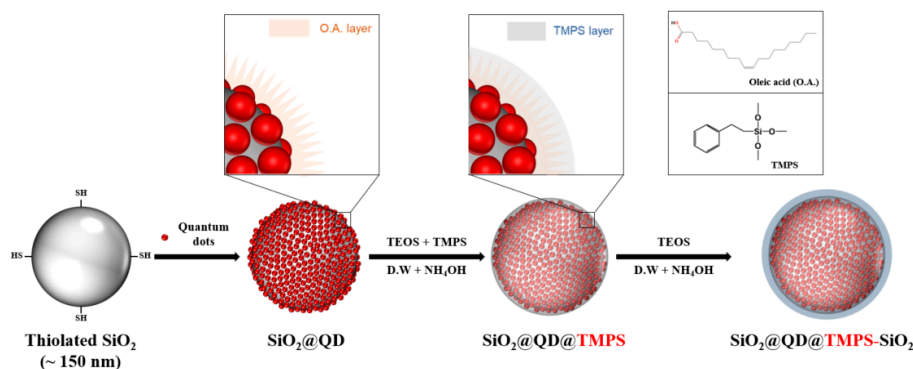
Figure 1. Synthesis of silica-encapsulated QD-embedded silica nanoparticles with TMPS (SiO_2@QD@TMPS-SiO_2).
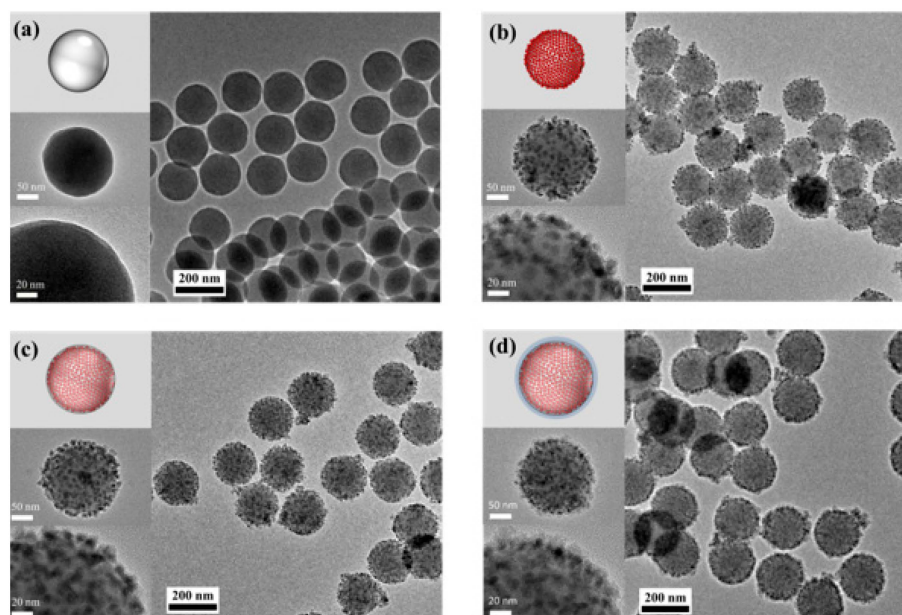
Figure 2. Illustrations and TEM images of each particle in the synthesis step: (**a**) SiO_2 NPs, (**b**) SiO_2@QD, (**c**) SiO_2@QD@TMPS, and (**d**) SiO_2@QD@TMPS-SiO_2.

3.2. Optical Properties of SiO_2@QD@TMPS-SiO_2

The optical properties of the fabricated NPs were evaluated. In principle, SiO_2@QD, SiO_2@QD@TMPS, and SiO_2@QD@TMPS-SiO_2 exhibited similar UV-Vis absorption and PL

spectra (Figure 3a,b) which originated from the QDs. These results show that the optical properties of the NPs (particularly the QDs) did not change after the silica encapsulation process. The particles mostly absorbed UV light at short wavelengths (~300 to 400 nm), and the degree of absorbance decreased with increasing wavelength.
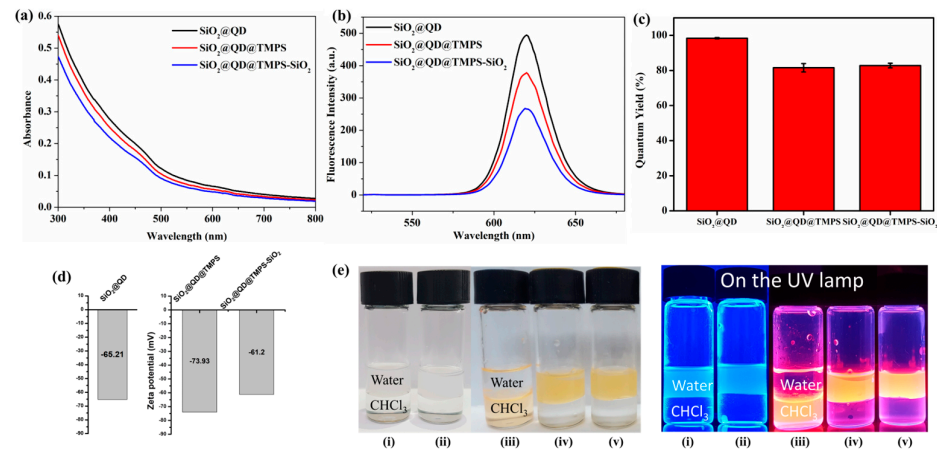
Figure 3. (**a**) UV−vis absorption spectra, (**b**) PL spectra, and (**c**) QYs for each step after the introduction of QDs during the synthesis of SiO_2@QD@TMPS-SiO_2. (**d**) Zeta potential of SiO_2@QD, SiO_2@QD@TMPS, and SiO_2@QD@TMPS−SiO_2. (**e**) Optical images under daylight (left) and UV light (right) of (i) SiO_2 NPs, (ii) Thiolated SiO_2 NPs, (iii) SiO_2@QD, (iv) SiO_2@QD@TMPS, and (v) SiO_2@QD@TMPS−SiO_2.

In terms of the PL spectra, the particles emitted light at a wavelength of 620 nm, which is the same as the light emitted from the individual QDs. Among the three types of NPs, SiO_2@QDs exhibited the highest PL intensity (494.59 in arbitrary units). In contrast, SiO_2@QD@TMPS-SiO_2 exhibited the lowest PL intensity (290.05 in arbitrary units). This phenomenon can be attributed to QD damage during fabrication. In addition, this originates from the thickness of the silica shell. The light that arrived at or was emitted from the SiO_2@QD did not undergo significant interference because the QDs of the SiO_2@QD were exposed. Meanwhile, in the cases of SiO_2@QD@TMPS and SiO_2@QD@TMPS-SiO_2 where the silica shell existed in the outer layer, the absorption or emission of light was interfered by the silica shell. Although the silica layer was relatively transparent, light scattering was inhibited by the silica shell.

To confirm the change in the QY after fabrication, the QYs of SiO_2@QD, SiO_2@QD@TMPS, and SiO_2@QD@TMPS-SiO_2 were also measured (Figure 3c). In the cases of SiO_2@QD and SiO_2@QD@TMPS, the QYs were similar (47.5% and 49.4%, respectively). Meanwhile, the QY decreased slightly after additional silica encapsulation with TEOS (49.4% and 41.3% for SiO_2@QD@TMPS and SiO_2@QD@TMPS-SiO_2, respectively). This was likely due to the interference of the outermost silica layer, as in the case of the PL intensity. Although the QY was reduced after additional silica encapsulation, the QY and PL intensity of SiO_2@QD@TMPS-SiO_2 were relatively good; in particular, the QY of SiO_2@QD@TMPS-SiO_2 was higher than that of QD[2], which was fabricated using the previous method [19]. The NPs in all phases were well dispersed, which is supported by the zeta potential data. As shown in Figure 3d, the high negative zeta potential values indicates that the NPs in all phases had good dispersion stability and were not aggregated [28].

3.3. Hydrophilicity of SiO_2@QD@TMPS-SiO_2

To confirm the silica encapsulation indirectly, hydrophilic properties of the NPs were evaluated at each fabrication step under daylight and UV light (Figure 3e). First, each mixtures containing SiO_2 NPs and thiolated SiO_2 NPs were well dispersed in the water phase and were not observed in the hydrophobic chloroform layer. These phenomena occurred owing to the functional groups which located onto the surface of each parti-

cle; silanol groups (Si-OH) on SiO$_2$ NPs and thiol groups (Si-SH) on thiolated SiO$_2$ NPs. Because these groups can be deprotonated in mild conditions, negative charges which enhance the colloidal stability and hydrophilicity of NPs could be existed onto the surface of NPs. When the QDs coated with oleic acid were attached to the surface of the thiolated SiO$_2$ NPs, SiO$_2$@QDs exhibited strong hydrophobicity owing to the oleyl group of the QD ligands and were transferred into the organic phase. In contrast, SiO$_2$@QD@TMPS and SiO$_2$@QD@TMPS-SiO$_2$ were well dispersed in the water phase. These results indicate that the outer functional groups were substituted from hydrophobic oleic acid to another hydrophilic functional groups. As mentioned at Section 3.1, the 2-phenylethyl group of TMPS, which has hydrophobic property was intercalated between oleic acid via hydrophobic interactions. Therefore, the exposed functional groups that were present onto the surface of SiO$_2$@QD@TMPS and SiO$_2$@QD@TMPS-SiO$_2$ should be the silanol group which originated from the hydrolysis of methoxy group. The dispersity of NPs which QDs were embedded (SiO$_2$@QD, SiO$_2$@QD@TMPS, and SiO$_2$@QD@TMPS-SiO$_2$) also could be confirmed by observing luminescence from the QDs under UV light irradiation.

3.4. Control of Silica Shell Thickness of SiO$_2$@QD@TMPS-SiO$_2$

According to the applications of NPs with optical properties, controlling of the thickness of outer silica shell should be necessary. With this reason, we tried to control the thickness of fabricated SiO$_2$@QD@TMPS-SiO$_2$ by adjusting the amount of TEOS used in the final silica encapsulation step. As shown in Figure 4a–c, the thickness of the silica shell layer increases with the increase in the amount of TEOS (25, 50, and 100 μL, respectively). Although the thickness of the silica layer varied, the morphology and other aspects of SiO$_2$@QD@TMPS-SiO$_2$ did not significantly differ, particularly in terms of the attachment of the QDs. Furthermore, varying the thickness of the silica layer did not significantly change the high negative zeta potential values of the NPs, which were presumed to maintain good dispersion (Figure S2).
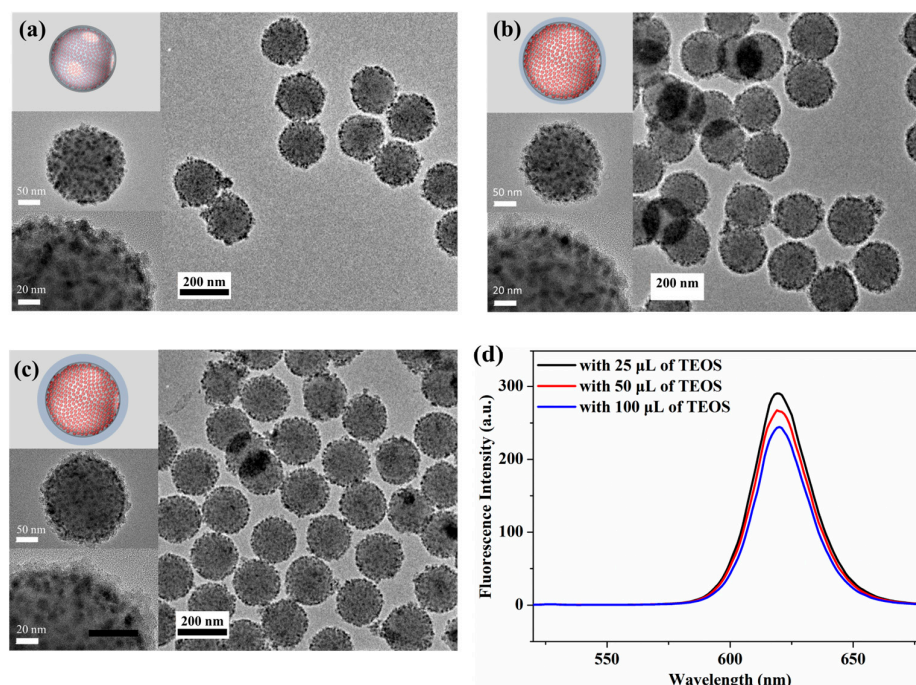
Figure 4. Illustration and TEM images of fabricated SiO$_2$@QD@TMPS-SiO$_2$ with different amounts of TEOS: (**a**) 25 μL (**b**) 50 μL, and (**c**) 100 μL. (**d**) PL spectra of fabricated nanoparticles.

The influence of the silica shell thickness on the optical properties of SiO$_2$@QD@TMPS-SiO$_2$ was evaluated. Regardless of the silica shell thickness, the PL spectra of SiO$_2$@QD@TMPS-SiO$_2$ were similar except for the maximum intensity (Figure 4d). The maximum fluorescence

intensity slightly decreased with an increasing of the silica shell thickness (from 290.05 to 244.25, in arbitrary units). As in the case of PL intensity, the QY of each particle decreased with increasing silica shell thickness (Figure S3, 42.6%, 41.3%, and 36.2%, respectively). These results may be related to the thickness of the outer silica shell layer. Even though the silica shell layer was almost transparent, the crossing of light, which came from the light source for excitation or fluorescence from QDs as an emission, could be inhibited via scattering or weak absorption. However, although the PL intensity and QY decreased in SiO_2@QD@TMPS-SiO_2 with a thick silica shell compared to the thin silica shell, SiO_2@QD@TMPS-SiO_2 with a thick silica shell can be used for other applications because it still has a relatively high PL intensity and QY, as compared to other QD–silica hybrid NPs.

3.5. Fabrication of Silica-Encapsulated Gold NP-Embedded Silica NPs with TMPS (SiO_2@Au_{2-NT}@SiO_2)

The silica encapsulation method using TMPS has also been adopted for noble metal NP-embedded silica NPs. Gold NP-assembled silica NPs (SiO_2@Au), which have shown excellent performance as near-infrared SERS nanoprobes, were selected as the target for silica encapsulation to ensure the feasibility of further surface modification [25]. As Raman label compound (RLC), 2-naphthalenethiol (2-NT), of which a single thiol group was conjugated at 2-position of naphthalene, was selected due to its strong hydrophobicity compared with another commonly used RLCs such as 4-mercaptobenzoic acid (4-MBA) or 4-aminothiophenol (4-ATP). To fabricate SiO_2@Au_{2-NT}, 2-NT was labeled onto the surface of SiO_2@Au. Because 2-NT was attached to the surface of SiO_2@Au via an interaction between thiol and Au, the outer-most functional group of SiO_2@Au_{2-NT} was the naphthyl group, which represents strong hydrophobicity. After labeling, SiO_2@Au_{2-NT} were encapsulated with a silica shell using TMPS and TEOS as silica precursors such as SiO_2@QD@TMPS. As in the case of oleyl groups of QDs, the naphthyl group interacted with the 2-phenylethyl group. However, differing from the oleyl groups, which can interact with the 2-phenylethyl group via hydrophobic interaction, naphthyl groups can interact with the 2-phenylethyl group via pi–pi interactions, which are stronger than simple hydrophobic interactions. After silica encapsulation using TMPS and TEOS, the silica shell layer was grown by using TEOS once more to fabricate SiO_2@Au_{2-NT}@SiO_2. As shown in Figure 5a, the overall morphology of the NPs does not change significantly, unlike silica encapsulation with TMPS. Notably, a thin silica shell layer can be observed in the outer layer of SiO_2@Au_{2-NT}@SiO_2 in the TEM image. These results indicate SiO_2@Au_{2-NT}@SiO_2 was successfully fabricated using TMPS.

3.6. Influence of Silica Encapsulation on the Optical Properties of SiO_2@Au_{2-NT}

To determine the influence of silica encapsulation with TMPS to the Raman signal intensity of the fabricated NPs, the Raman spectra of SiO_2@Au_{2-NT} were acquired before and after silica encapsulation (SiO_2@Au_{2-NT} and SiO_2@Au_{2-NT}@SiO_2, respectively). As shown in Figure 5b, the spectral patterns of SiO_2@Au_{2-NT} and SiO_2@Au_{2-NT}@SiO_2 were largely the same, and representative peaks were observed at 1065, 1378, 1565, and 1619 cm^{-1} for both these particles. In particular, the peaks at 1565 and 1619 cm^{-1} are assigned to the aromatic ring stretching mode of the 2-NT unit, which means that 2-NT exists on the surface of SiO_2@Au regardless of the TMPS treatment [29,30]. Moreover, the Raman signal intensities of SiO_2@Au_{2-NT} and SiO_2@Au_{2-NT}@SiO_2 at 1619 cm^{-1} were similar (5204 vs. 4146, in arbitrary units) at the same particle concentration. These results indicate that the silica encapsulation of SiO_2@Au_{2-NT} with TMPS did not influence the optical properties, specifically the Raman signal intensity.
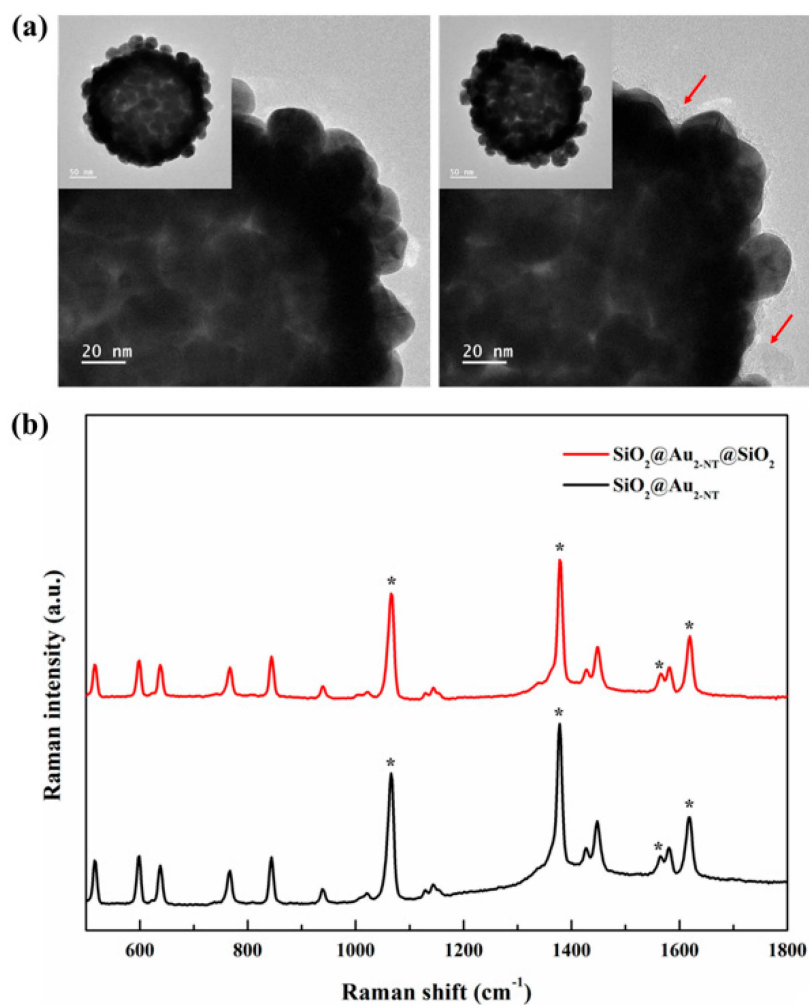
Figure 5. TEM images of (**a**) $SiO_2@Au_{2\text{-}NT}$ (left) and $SiO_2@Au_{2\text{-}NT}@SiO_2$ (right). The red arrow indicates the silica shell. (**b**) Raman spectra of $SiO_2@Au_{2\text{-}NT}$ and $SiO_2@Au_{2\text{-}NT}@SiO_2$. The "*" indicates the representative peaks of 2-NT.

4. Conclusions

We introduced a novel generalizable method for the encapsulation of NP-embedded silica NPs with TMPS and fabricated $SiO_2@QD@TMPS\text{-}SiO_2$ NPs and $SiO_2@Au_{2\text{-}NT}@SiO_2$ NPs using the introduced method. In the case of the $SiO_2@QD@TMPS\text{-}SiO_2$ NPs, TMPS interacted with hydrophobic oleic acid that was attached to the surface of the QD and formed a silica shell layer without ligand exchange. The PL and QY of $SiO_2@QD@TMPS\text{-}SiO_2$ NPs were not significantly lower than those of $SiO_2@QD$. The thickness of the outer silica shell was controlled by adjusting the amount of TEOS used during the silica shell formation step, which was the last step in the fabrication. Silica encapsulation with TMPS was also applied to $SiO_2@Au_{2\text{-}NT}$ NPs, and the outer silica shell was formed successfully without any significant change of morphology of NPs. Raman signal spectra of the NPs also did not change significantly during silica encapsulation. Based on these results, we expect that the proposed silica encapsulation method using TMPS can be applied to not only other hydrophobic RLC-labeled $SiO_2@Au$ NPs, but also to NPs with hydrophobic surfaces.

Supplementary Materials: The following supporting information can be downloaded at: https://www.mdpi.com/article/10.3390/nano13142145/s1, Figure S1: Histogram of particle size distribution of SiO_2 NPs, Figure S2: Zeta potential of $SiO_2@QD@TMPS\text{-}SiO_2$ with different amount of TEOS, Figure S3: Quantum yield of fabricated $SiO_2@QD@TMPS\text{-}SiO_2$ with different amount of TEOS.

References

1. Takagahara, T.; Takeda, K. Theory of the quantum confinement effect on excitons in quantum dots of indirect-gap materials. *Phys. Rev. B* **1992**, *46*, 15578–15581. [CrossRef] [PubMed]
2. Zorman, B.; Ramakrishna, M.V.; Friesner, R.A. Quantum Confinement Effects in CdSe Quantum Dots. *J. Phys. Chem.* **1995**, *99*, 7649–7653. [CrossRef]
3. Amendola, V.; Pilot, R.; Frasconi, M.; Maragò, O.M.; Iatì, M.A. Surface plasmon resonance in gold nanoparticles: A review. *J. Phys. Condens. Matter* **2017**, *29*, 203002. [CrossRef] [PubMed]
4. Ghosh, S.K.; Pal, T. Interparticle Coupling Effect on the Surface Plasmon Resonance of Gold Nanoparticles: From Theory to Applications. *Chem. Rev.* **2007**, *107*, 4797–4862. [CrossRef]
5. Pham, X.-H.; Park, S.-M.; Ham, K.-M.; Kyeong, S.; Son, B.S.; Kim, J.; Hahm, E.; Kim, Y.-H.; Bock, S.; Kim, W.; et al. Synthesis and Application of Silica-Coated Quantum Dots in Biomedicine. *Int. J. Mol. Sci.* **2021**, *22*, 10116. [CrossRef] [PubMed]
6. Liu, S.H.; Han, M.Y. Synthesis, Functionalization, and Bioconjugation of Monodisperse, Silica-Coated Gold Nanoparticles: Robust Bioprobes. *Adv. Funct. Mater.* **2005**, *15*, 961–967. [CrossRef]
7. Zhang, B.; Gong, X.; Hao, L.; Cheng, J.; Han, Y.; Chang, J. A novel method to enhance quantum yield of silica-coated quantum dots for biodetection. *Nanotechnology* **2008**, *19*, 465604. [CrossRef]
8. Zhang, Y.; Li, X.; Xue, B.; Kong, X.; Liu, X.; Tu, L.; Chang, Y. A facile and general route to synthesize silica-coated SERS tags with the enhanced signal intensity. *Sci. Rep.* **2015**, *5*, 14934. [CrossRef]
9. Aubert, T.; Soenen, S.J.; Wassmuth, D.; Cirillo, M.; Van Deun, R.; Braeckmans, K.; Hens, Z. Bright and Stable CdSe/CdS@SiO$_2$ Nanoparticles Suitable for Long-Term Cell Labeling. *ACS Appl. Mater. Interfaces* **2014**, *6*, 11714–11723. [CrossRef]
10. Selvan, S.T.; Tan, T.T.; Ying, J.Y. Robust, Non-Cytotoxic, Silica-Coated CdSe Quantum Dots with Efficient Photoluminescence. *Adv. Mater.* **2005**, *17*, 1620–1625. [CrossRef]
11. Kirchner, C.; Liedl, T.; Kudera, S.; Pellegrino, T.; Muñoz Javier, A.; Gaub, H.E.; Stölzle, S.; Fertig, N.; Parak, W.J. Cytotoxicity of Colloidal CdSe and CdSe/ZnS Nanoparticles. *Nano Lett.* **2005**, *5*, 331–338. [CrossRef]
12. Pham, X.-H.; Tran, V.-K.; Hahm, E.; Kim, Y.-H.; Kim, J.; Kim, W.; Jun, B.-H. Synthesis of Gold-Platinum Core-Shell Nanoparticles Assembled on a Silica Template and Their Peroxidase Nanozyme Properties. *Int. J. Mol. Sci.* **2022**, *23*, 6424. [CrossRef]
13. Abu El-Soad, A.M.; Lazzara, G.; Pestov, A.V.; Tambasova, D.P.; Antonov, D.O.; Cavallaro, G.; Kovaleva, E.G. Grafting of (3-Chloropropyl)-Trimethoxy Silane on Halloysite Nanotubes Surface. *Appl. Sci.* **2021**, *11*, 5534. [CrossRef]
14. Santhamoorthy, M.; Ramkumar, V.; Thirupathi, K.; Gnanasekaran, L.; Karuppannan, V.; Phan, T.T.V.; Kim, S.-C. L-lysine Functionalized Mesoporous Silica Hybrid Nanoparticles for pH-Responsive Delivery of Curcumin. *Pharmaceutics* **2023**, *15*, 1631. [CrossRef]
15. Kim, J.; Lee, S.; Lee, Y.K.; Seong, B.; Kim, H.-M.; Kyeong, S.; Kim, W.; Ham, K.; Pham, X.-H.; Hahm, E.; et al. In Vitro Tracking of Human Umbilical Vein Endothelial Cells Using Ultra-Sensitive Quantum Dot-Embedded Silica Nanoparticles. *Int. J. Mol. Sci.* **2023**, *24*, 5794. [CrossRef]
16. Ham, K.-M.; Kim, M.; Bock, S.; Kim, J.; Kim, W.; Jung, H.S.; An, J.; Song, H.; Kim, J.-W.; Kim, H.-M.; et al. Highly Bright Silica-Coated InP/ZnS Quantum Dot-Embedded Silica Nanoparticles as Biocompatible Nanoprobes. *Int. J. Mol. Sci.* **2022**, *23*, 10977. [CrossRef]
17. Bock, S.; Kim, H.-M.; Kim, J.; An, J.; Choi, Y.-S.; Pham, X.-H.; Jo, A.; Ham, K.-m.; Song, H.; Kim, J.-W.; et al. Lateral Flow Immunoassay with Quantum-Dot-Embedded Silica Nanoparticles for Prostate-Specific Antigen Detection. *Nanomaterials* **2022**, *12*, 33. [CrossRef]
18. Kim, H.-M.; Oh, C.; An, J.; Baek, S.; Bock, S.; Kim, J.; Jung, H.-S.; Song, H.; Kim, J.-W.; Jo, A.; et al. Multi-Quantum Dots-Embedded Silica-Encapsulated Nanoparticle-Based Lateral Flow Assay for Highly Sensitive Exosome Detection. *Nanomaterials* **2021**, *11*, 768. [CrossRef]
19. Jun, B.-H.; Hwang, D.W.; Jung, H.S.; Jang, J.; Kim, H.; Kang, H.; Kang, T.; Kyeong, S.; Lee, H.; Jeong, D.H.; et al. Ultrasensitive, Biocompatible, Quantum-Dot-Embedded Silica Nanoparticles for Bioimaging. *Adv. Funct. Mater.* **2012**, *22*, 1843–1849. [CrossRef]

20. Kim, H.-M.; Kim, J.; Bock, S.; An, J.; Choi, Y.-S.; Pham, X.-H.; Cha, M.G.; Seong, B.; Kim, W.; Kim, Y.-H.; et al. Silver-Assembled Silica Nanoparticles in Lateral Flow Immunoassay for Visual Inspection of Prostate-Specific Antigen. *Sensors* **2021**, *21*, 4099. [CrossRef]

21. Kim, H.-M.; Jeong, S.; Hahm, E.; Kim, J.; Cha, M.G.; Kim, K.-M.; Kang, H.; Kyeong, S.; Pham, X.-H.; Lee, Y.-S.; et al. Large scale synthesis of surface-enhanced Raman scattering nanoprobes with high reproducibility and long-term stability. *J. Ind. Eng. Chem.* **2016**, *33*, 22–27. [CrossRef]

22. Le, T.-H.; Kim, S.; Chae, S.; Choi, Y.; Park, C.S.; Heo, E.; Lee, U.; Kim, H.; Kwon, O.S.; Im, W.B. Zero reduction luminescence of aqueous-phase alloy core/shell quantum dots via rapid ambient-condition ligand exchange. *J. Colloid Interface Sci.* **2020**, *564*, 88–98. [CrossRef] [PubMed]

23. Yoo, H.; Woo, K. Direct Hybridization of Hydrophobic Nanocrystals with Colloidal Silica via van der Waals Force. *J. Phys. Chem. Lett.* **2018**, *9*, 2106–2112. [CrossRef]

24. Stöber, W.; Fink, A.; Bohn, E. Controlled growth of monodisperse silica spheres in the micron size range. *J. Colloid Interface Sci.* **1968**, *26*, 62–69. [CrossRef]

25. Bock, S.; Choi, Y.-S.; Kim, M.; Yun, Y.; Pham, X.-H.; Kim, J.; Seong, B.; Kim, W.; Jo, A.; Ham, K.-M.; et al. Highly sensitive near-infrared SERS nanoprobes for in vivo imaging using gold-assembled silica nanoparticles with controllable nanogaps. *J. Nanobiotechnol.* **2022**, *20*, 130. [CrossRef]

26. Seong, B.; Bock, S.; Hahm, E.; Huynh, K.-H.; Kim, J.; Lee, S.H.; Pham, X.-H.; Jun, B.-H. Synthesis of Densely Immobilized Gold-Assembled Silica Nanostructures. *Int. J. Mol. Sci.* **2021**, *22*, 2543. [CrossRef]

27. Duff, D.G.; Baiker, A.; Edwards, P.P. A new hydrosol of gold clusters. 1. Formation and particle size variation. *Langmuir* **1993**, *9*, 2301–2309. [CrossRef]

28. Ramasamy, M.; Yi, D.K.; An, S.S.A. Enhanced detection sensitivity of Escherichia coli O157: H7 using surface-modified gold nanorods. *Int. J. Nanomed.* **2015**, *10* (Suppl S1), 179–190.

29. Agarwal, N.R.; Lucotti, A.; Tommasini, M.; Neri, F.; Trusso, S.; Ossi, P.M. SERS detection and DFT calculation of 2-naphthalene thiol adsorbed on Ag and Au probes. *Sens. Actuators B Chem.* **2016**, *237*, 545–555. [CrossRef]

30. Harun, N.A.; Horrocks, B.R.; Fulton, D.A. Enhanced Raman and luminescence spectra from co-encapsulated silicon quantum dots and Au–Ag nanoalloys. *Chem. Commun.* **2014**, *50*, 12389–12391. [CrossRef]